HHS Public Access

Author manuscript

Nat Neurosci. Author manuscript; available in PMC 2010 October 01.

Published in final edited form as:

Nat Neurosci. 2010 April ; 13(4): 495–500. doi:10.1038/nn.2496.

Intention and Attention: Different functional roles for LIPd and LIPv

YQ Liu[1], **EA Yttri**[1], and **LH Snyder**[1]

[1]Department of Anatomy and Neurobiology, Washington University School of Medicine, 660 S. Euclid Ave, St. Louis, Missouri 63110, USA

Abstract

Establishing the circuitry underlying attentional and oculomotor control is a longstanding goal of systems neuroscience. The macaque lateral intraparietal area, LIP, has been implicated in both processes, but numerous studies have produced contradictory findings. Anatomically, LIP consists of a dorsal and ventral subdivision, yet the functional significance of this division remains unclear. We co-injected muscimol, a GABAa agonist, and manganese, an MR-lucent paramagnetic ion, into different portions of LIP, testing the effect of the resulting reversible inactivation on saccade planning and attention, and visualized each injection using anatomical MRI. We find that LIPd is primarily an oculomotor planning region, while LIPv contributes to both attentional and oculomotor processes. Additional testing reveals that, even within LIPv, the two functions are dissociable. Thus our novel muscimol+Mn-MRI technique establishes clear structure-function relationships that distinguish LIPv from LIPd, and reveals dissociable circuits for attention and eye movements in the posterior parietal cortex.

The goal of this study was to distinguish between circuits dedicated to general perception and circuits specialized for directing particular movements. Area LIP has been implicated in both saccade planning and attentional processing, with conflicting evidence from single unit recording[1]-[4], intracortical microstimulation[5], [6], anatomical studies[7]-[10], surgical lesions[11], and reversible inactivation[12]-[15]. Ambiguities arise because attention and eye movements are tightly coupled. Although attention can be disengaged from the point of fixation[16], primates usually look at objects of interest[17]. However, even when subjects attend to a peripheral target without looking directly at it, oculomotor planning activity likely occurs nonetheless[18]-[20]. We aim to understand the role of LIP in these processes and whether attention and oculomotor planning rely on shared or distinct neuronal substrates.

Although LIP is often treated as a whole, it is in fact composed of two separate areas, the dorsal and ventral lateral intraparietal areas (LIPd and LIPv). The distinction is based on patterns of myelination, connectivity, and immunohistochemistry[21]-[23]. LIPv, deep in the

Correspondence should be addressed to L.Y.Q. (yuqing@eye-hand.wustl.edu)..

Author Contributions L.Y.Q. performed all aspects of this study including the experimental design, data collection of two monkeys, analysis, and writing the manuscript. Y.E.A. assisted in data collection and analysis. L.H.S. oversaw the experiments and assisted in data analysis and manuscript preparation.

lateral bank of the intraparietal sulcus (IPS), is characterized by dense myelination while LIPd, superficial to LIPv, is lightly myelinated[22, 23]. LIPv is more strongly connected with V3, PIP, and PO, while LIPd is more strongly connected with V4, V4t, TEa/m, TPOr, and area 45[21]. Both are reciprocally connected to FEF[21, 23]. Conflicting results regarding the role of LIP could occur if LIPd and LIPv serve different functions and previous studies sampled them differently. To address this possibility, we tested whether LIPd and LIPv play different roles in oculomotor and attentional processing.

Single unit recording is frequently used to explore structure-function relationships. However, the determination of what structure one is recording from is often partially based on the functional properties being recorded, and this circularity can lead to uncertainty. This can be ameliorated by reconstructing the recording sites based on post mortem landmarks, reconstructing the electrode trajectories based on stereotaxic data, or directly imaging the electrode *in* vivo[24].

Recording techniques coupled with recording site reconstruction can demonstrate correlations between neural activity and particular task conditions, but do not directly address the causal role neurons may play in behavior. More information can be obtained by lesioning the area and observing in what tasks deficits arise. As with unit recording, proper interpretation requires accurate localization of the lesion. We achieve this by coinjecting muscimol with manganese. Muscimol, a $GABA_a$ agonist, increases local inhibition and thereby attenuates local activity. The manganese can be imaged using magnetic resonance imaging[25], providing direct *in vivo* visualization of the injection site.

We find that LIPd and LIPv play different roles in saccade planning and covert attention. Lesions of LIPd affect saccades but not search, while lesions of LIPv affect both saccades and search. Our findings further indicate that oculomotor and attentional processes in LIPv can be dissociated at the neural circuit level.

Results

LIP lesions impair both saccades and search

After mapping out LIP based on standard functional criteria (see Methods), we performed 35 reversible inactivations in 3 animals using 1 – 4 μl of 8.0 mg/ml muscimol mixed with 19.8 mg/ml tetrahydrate manganese chloride ($MnCl_2(H_2O)_4$). We tested the effects of each lesion on a standard memory-guided saccade task and a visual search task (Fig. 1a). A visual search paradigm is useful for measuring attentional effects because visual search in general requires the use of limited resources for information processing[26], and attention is thought to operate most strongly when distinguishing a target from distractors[27].

The muscimol lesions affected both saccadic and search performance, with the former occurring about twice as frequently as the latter. Figure 1 shows two example injections, one with a saccade effect (Fig. 1b) and the other with a saccade and search effect (Fig. 1c). A 4 μl injection close to the gyral surface (**Fig. 1b**, inset) increased saccade reaction time (RT) by 10.2 ms compared to control sessions (P = 7.6e-04, two-sided Welch's t-test). This injection did not significantly affect saccade error rate (experimental minus control rates =

0.3% [P = 1.0], two-sided Fisher test; **Fig. 1b**, grey). There were small improvements in search error rate (−5.2% [P = 0.28], two-sided χ^2 test) and search RT (−4.8 ms [P=0.06]) (**Fig. 1b**,black). In contrast, a second injection of 3 μl, deeper in the sulcus, (**Fig. 1c**, inset) not only significantly impaired saccades (7.5 ms slowing [P = 0.024]; change in error rate not significant [P=0.28]) but also impaired search (+18.1% ER [P < 2e-08]; change in RT not significant [P=0.78]). Here and throughout the rest of this paper, we report lesion effects on saccades and search only to contralateral targets, except where otherwise noted.

Search is impaired by LIPv but not LIPd lesions

The two example injections, one shallow and one deep into the IPS sulcus (Fig. 1b and c), had different effects on visual search. To test for a systematic effect of lesion depth on search, we plotted error rate against normalized depth for each injection (see Methods and Fig. 2a). Anatomical data suggest that the LIPd/v boundary lies at 53% of full sulcal depth[22] (6.8 mm for our animals; see Methods). No injections above this border (**Fig. 2**, vertical dashed line, left) produced significant search effects, while 72% (13/18) of deeper injections significantly increased search errors (P<.05). This was also true for the data from each of the three animals considered individually (Table 2): no shallow injections affected search, while 5/7, 6/8 and 2/3 of the deep injections impaired search. The difference in errors between shallow (LIPd: −0.2 ± 1.4% [P = 0.86]) and deep (LIPv: 15.7 ± 3.4% [P = 6.1e-05]) injections was highly significant (P = 5.3e-05, two-sided permutation test). There was a similar though non-significant trend in search RT, with LIPd lesions having almost no effect (−0.65 ms, P=0.6) while LIPv lesions slowed responses by 6.6 ms (P = 0.35). Thus LIPv but not LIPd lesions impaired visual search.

In contrast to search effects, saccade effects occurred after both LIPd and LIPv lesions. Memory-guided saccades were impaired (either slowed RT or increased error rate, P < 0.025, two-sided Welch's t-test and χ^2 test) in 12 of 17 (70.6%) LIPd injections and 13 of 18 (72.2%) LIPv injections (**Fig. 3a and b**, grey), and there was no linear trend in the effect size as a function of depth (Fig. 2b: Pearson correlation coefficient r = −0.031, P = 0.86). For comparison, the search data do show a linear trend (r = 0.64, P = 0.0001). At a population level, the effect on mean adjusted RT (a measure combining RT and error effects; see Supplementary Information) for saccades was similar for LIPd (11.1 ± 1.8 ms [P = 9.2e-05]) and LIPv (10.1 ± 2.0 ms [P = 5.3e-05]). Similar effects were found on visually-guided saccades in both LIPd (n = 2, mean RT effect = 8.3 ms) and LIPv (n = 6, RT effect = 9.8 ± 4.9 ms [P = 0.094]), demonstrating that the deficit was not specific to working memory. Effects on saccade accuracy, precision, duration, and error rate were small or absent in both LIPd and LIPv (see Supplementary information).

Directional effects on saccades and search

The distinction between LIPd and LIPv was also apparent when individual target directions were considered. LIPd lesions did not affect search errors for targets in any single direction (mean = −2.3%, all P > 0.4 for increase of errors, **Fig. 3e**, solid black line), while LIPv lesions significantly increased search errors for all three contralateral targets (12.3% [P = 0.0004]; 13.8% [P = 0.0009]; and 12.6% [P = 0.006], respectively; **Fig. 3f**, solid black line). Unlike search, saccades were impaired by lesions of either area, especially for contralateral

and upwards directions (LIPd: 14.9, 8.7, 12.9, and 7.4 ms, all $P < 0.05$, **Fig. 3c**, solid grey line; LIPv: 10.6, 13.4, 9.3, and 7.0 ms, all $P < 0.08$, **Fig. 3d**, solid grey line). Lesions of LIPd and LIPv had similar effects on saccades in each individual direction (t-tests, all $P >= 0.2$) as well as on the pooled measure ($P = 0.72$).

The lesion effects were consistent across each of the three animals (Table 1 and 2). All three animals showed markedly elevated contralateteral saccade RT effects in both areas, significant in two animals. In each of the three animals the contralateral search effect was markedly elevated in LIPv (significant in two) and non-significant (small or negative) in LIPd. A two-way [direction × monkey] ANOVA revealed no main effect of monkey either on the contralateral saccade RT effect (LIPd: $F(2) = 1.7$, $P = 0.2$; LIPv: $F(2) = 1.9$, $P = 0.16$) or on the contralateral search error effect (LIPd: $F(2) = 0.52$, $P = 0.6$; LIPv: $F(2) = 0.23$, $P = 0.79$).

Lesions effects depend on eye position for search but not for saccades

The retinotopic responses of LIP neurons are gain modulated by eye position[28]. To test if eye position might modulate lesion effects, two animals performed the saccade and search tasks after a subset of injections with all visual stimuli, including the initial fixation target, displaced either 5° to the left or right of straight ahead (Fig. 4a). Saccade RTs were slowed to a similar extent regardless of eye position in LIPd and LIPv (Supplementary table 2 and grey bars in Fig. 4b and c). This was true for each individual injection, with significant effects of eye position on saccade RT occurring at only 4/9 LIPd sites [2 increased and 2 decreased RTs with contralateral eye position] and 1/9 LIPv sites [decreased RT with contralateral eye position], and also true for the population (LIPd: 5.7 ± 3 ms versus 5.8 ± 1.6 ms, difference $P = 0.96$, paired t-test; LIPv: 10 ± 2.5 ms versus 8.0 ± 2.9, difference $P = 0.24$). There was no search effect in LIPd for either eye position (−2.1 ± 1.4% [$P = 0.18$]; −0.55 ± 1.4% [$P = 0.7$], **Fig. 4b**, black bars). In LIPv, however, the error rate for search more than doubled for contralateral compared to ipsilateral eye position (11 sites tested: 16.8 ± 5.5% versus 5.4 ± 2.2%, difference $P = 0.034$, paired t-test; **Fig. 4c**, black bars). At the individual injection level, 10 out of 11 LIPv injections resulted in more search errors with contralateral compared with ipsilateral eye positions, and of those, 6 of the 11 were significantly greater ($P < 0.02$, two-sided chi-square test or Fisher exact test). Thus, the search effect depends on initial eye position in LIPv, while the saccade effect is independent of eye position in both areas.

Lesion overlap map

To further characterize the anatomical locus of the search effect, we constructed 3-D (Fig. 5a and b) and 2-D (Fig. 5c) lesion overlap maps (see Supplementary methods) showing the 8 search-positive and 12 search-negative lesions from the two fascicularis monkeys. Search-positive effects (**Fig. 5b and c**, yellow-red) result from injections in the ventral (deep) portion of the IPS, while search-negative effects (**Fig. 5a and c**, green-blue) result from dorsal (superficial) injections in the lateral bank, directly above the search positive area. The voxels that are most frequently involved in search-positive or search-negative effects are separated by 3.0 mm. These results support the conclusion that search is impaired by LIPv but not LIPd injections.

Control experiments

To rule out alternative explanations for the origin of search effects, we performed eight control injections into the medial bank of the IPS (Fig. 6a and b). Neither large (n = 4, Fig. 6a) nor focal (n = 5, Fig. 6b) medial bank injections impaired search (mean effect = −0.36% [P=0.75] and 1.2% [P = 0.56], respectively). To test if search effects are produced by large inactivations independent of their locations, we picked 5 large LIPd injections with additional involvement of 7a (Fig. 6c) and inspected their effects on search and saccades. These injections all significantly impaired saccades (all P <= 0.03, mean effect on adjusted RT = 11.3 ms [P = 0.06]) but had no effect on search (mean = 0.12% [P = 0.94]). Thus our control experiments confirm that the search effect was specific to lesions of the ventral portion of the lateral bank in the IPS.

In addition, we examined whether our lesion effects were specifically related to GABA modulation. A manganese-only injection (3.0 μl) was made into both LIPd and LIPv (Supplementary fig. 4a). There was a slight non-significant improvement on saccade RT (−2.2 ms [P = 0.63]) and error rate (−1.7% [P = 0.9]; **Supplementary fig. 4b**, green). Search performance was also unaffected (3.0 ms [P = 0.46] and −0.4% [P = 1.0]; **Supplementary fig. 4b**, red). In contrast, a 1.0 μl muscimol injection into LIPv without manganese impaired both saccades (30.2 ms [P = 4e − 06]; 8.9% [P =0.053]) and search (−4.8 ms [P = 0.15]; 16.7% [P = 8e − 08]). A 3.0 μl muscimol alone injection placed in LIPd impaired saccades (1.7 ms [P =0.4]; 12.9% [P = 0.0001]) but not search (−1.8 ms [P = 0.25]; −3.0% [P = 0.44]). The results of these control injections suggest that the lesion effects observed in our experiments were specifically due to the modulation of GABAergic inhibitory circuits in LIPd or LIPv, and that injecting manganese alone into the parietal cortical tissue has minimal effects on saccade and search performance.

Discussion

Together these results show that well-localized injections of the $GABA_a$ agonist muscimol into LIPd specifically impair saccades but leave search intact. In contrast, well-localized injections into LIPv impair both search and saccades. There have been two previous reversible inactivation studies of LIP. Our finding of saccade deficits in LIPd and LIPv is consistent with the results of Li et al.[14] and our finding of search deficits in LIPv is consistent with the major finding of Wardak et al.[13], [15], although Li et al. and Wardak et al. neither distinguished between LIPd and LIPv, nor tested for an anatomical gradient of their lesion effects. Wardak and colleagues reported no significant effect of LIP lesions on saccade RT at the population level, but did not report data from individual injections.

The visual search paradigm that we employed is the “difficult feature search” of Wardak et al.[13], in which search time depends on the number of distractors. We confirmed that this was the case in our animals prior to collecting lesion data, and then compared search performance after each lesion in the presence and absence of distractors. This controls for effects of saccades per se and isolates a cost that is ascribed to the role of attention. Because visual search involves many different processes, our results and those of previous studies could conceivably reflect an impairment of, for example, shape processing[29]. However, the

most likely explanation for the search effect that we see in LIPv is an impairment in attentional control.

Our muscimol plus manganese-enhanced MRI technique allows us to distinguish the different functional roles of dorsal and ventral LIP. This technique can significantly improve the traditional reversible inactivation technique for closely spaced areas and regions in which areal boundaries are not obvious, and to resolve controversial issues regarding the functions of other regions such as DLPFC.

Areal distinctions

LIPd and LIPv have not been well-studied as separate areas. While they have much in common, they show differences in connectivity and physiology. Anatomically, LIPv is more strongly connected with V3, PIP, and PO, while LIPd is more strongly connected with V4, V4t, TEa/m, TPOr, and area 45[21]. Both areas are connected to frontal areas close to the FEF[9, 21, 23], with LIPv more strongly connected with the caudal periarcuate area[23] and ventral frontal eye fields (areas 45, 6Vam)[21]. While LIPd is more strongly connected with the rostral periarcuate area (intermediate area 8)[23] and dorsal frontal eye field (8Ac, 8As)[21], some authors report overall stronger connections from LIPv to FEF[30]. FEF has been traditionally viewed as an oculomotor structure, but it has been recently implicated in attentional processing [31-33]. This dual role is consistent with our finding of both saccade and search effects after LIPv lesions. LIP also has direct projections to the superior colliculus[7] (SC). Like FEF, SC has been traditionally viewed as an oculomotor structure, but has also been recently implicated in attentional processing[34, 35]. The LIP neurons projecting to FEF and SC are intermingled[36], but there appears to be a stronger projection to the intermediate and deep layers of the SC from deeper areas in the lateral bank, approximately corresponding to LIPv[7]. In summary, LIPv, when compared to LIPd, has stronger connections to FEF and SC and weaker connections to V4. This is surprising given our results and the classic view of FEF and SC as oculomotor-related and V4 as attention-related. This surprise is mitigated, however, by the fact that SC, FEF, and V4 all show both oculomotor and attentional effects[34, 35, 37], and that FEF is itself strongly connected with V4[10, 30]. Furthermore, it has been previously suggested that LIPv is involved in complex cognitive functions such as integrating sensory evidence and engaging and disengaging attention[38-40]. Functionally, single unit recording studies have suggested that LIPv represents the periphery while LIPd represents the fovea[9, 41], but we did not find evidence for impaired foveal stability after either LIPd or LIPv lesions (see Supplementary information).

Functional specificity at the areal level

There has been a long-standing debate about whether LIP has a specific oculomotor role[1, 2, 5, 12, 14] or plays a role in allocating attention, perhaps by providing a general salience map of visual space[3, 4, 6, 13, 15]. A number of studies have attempted to separate saccadic from attentional processing[4, 20]. The locus of attention can be continuously tracked using psychophysical techniques, but saccadic intention is much more difficult to measure. Activity in LIP tracks the time course of attention[4], predicts the goal and latency of upcoming saccades under conditions of free visual search[42] but not when a task-irrelevant

stimulus appears near the end of the delay period of a memory-guided delayed saccade[43], and distinguishes between targets and distractors during visual search[44]. These findings suggest that LIP is involved in both attention and saccade intention. Our lesion data confirms this, consistent with previous studies showing an intimate relationship between the saccade and attention systems at the level of both behavior[17] and neural circuitry[18], [19].

The effects we observed of LIP lesions on saccades and search were very small but reliable, e.g. 5 – 10 ms increases in latency. The search effects shown in our data and reported by Wardak et al.[13] were comparable to those of FEF inactivations[45], but the saccade effects were at least an order of magnitude smaller than those of FEF[45], [46] and SC inactivations[47], and lesions in these areas also impaired saccade metrics. This is consistent with the notion that LIP helps specify saccadic goals but, unlike FEF and SC, does not play a direct role in generating the saccade itself. In addition, parallel pathways that bypass LIP may exist for specifying saccade goals, which could compensate for the loss of function after LIP lesions. Finally, SC and, to a lesser extent, FEF are more highly topographically organized than LIP, so circumscribed lesions may have pronounced focal effects in SC and FEF, and more diffuse effects in LIP.

Functional specificity at the neural circuit level

Our data suggest that there may be separate neural substrates for oculomotor and attentional functions in LIPv, similar to what has been found in FEF[31], [32]. LIPd and LIPv lesions affected saccade RT more reliably than the saccade error rate, while LIPv lesions affected search error rate more strongly than reaction time. More importantly, eye position modulates the search effect but not the saccade effect (Fig. 4c). The lack of an eye position effect on saccades is consistent with previous results from Li & Andersen[48], while the eye position effect on visual search is consistent with the fact that hemineglect in humans is often modulated by eye position[49], [50]. Therefore we propose that there are two intermingled cell populations in LIPv, similar to what has been found in FEF[31], with one group of cells involved in saccade planning and the other involved in spatial attention.

Conclusion

In summary, our findings reveal different functional roles for the two subdivisions of LIP: LIPd is primarily an oculomotor planning region and LIPv is involved in both oculomotor and attentional processing. Thus oculomotor processing can exist independent of attentional processing within the posterior parietal cortex (LIPd), but the two processes can also operate side-by-side within the same cortical area (LIPv). Furthermore, when both processes are present in the same area, they appear to be subserved by independent neural elements (LIPv and FEF). This architecture may provide a flexible neuronal substrate for switching between coupling and decoupling of covert attention and eye movements[18], [19], [31].

METHODS

Three adult male macaque monkeys (two *Macaca fascicularis*, monkey Q and W; one *Macaca mulatta*, monkey G) were used in the current study. All procedures conformed to

the *Guide for the Care and Use of Laboratory Animals* and were approved by the Washington University Institutional Animal Care and Use Committee.

Delineation of LIP

We localized LIP in four hemispheres of three monkeys using MRI and single neuron recording. LIP was defined as a zone in the lateral bank of the IPS, close to the bend in the sulcus, containing a high proportion of cells with a brisk phasic response to onset of a visual target within the receptive field and significantly elevated activity during the delay period of a memory-guided saccade task (Supplementary fig. 1).

Injections

8 mg/ml muscimol and 0.1 M manganese (19.8 mg/ml $MnCl_2.(H_2O)_4$) in sterile water was injected at 0.1 μl/min using a microinjection pump (Harvard Apparatus HA11D). A total of 8 – 32 μg muscimol (median: 16 μg) was injected per experiment. Injections were made through a chamber mounted over LIP using a custom assembly consisting of 33-gauge hypodermic tubing connected to a 25 μl Hamilton syringe. Injection coordinates were selected based on pre-injection mapping experiments (see Supplemental fig. 1) and on animal-specific MRI atlases. For each experiment, 1 or 2 μl of muscimol+Mn was injected at 1 to 4 sites along one or two injection tracks, for a total volume of 1 – 4 μl per experiment.

The volumes of injections placed in the two areas were comparable (mean ± s.d.: 2.6 ± 0.9 [mode: 2] μl for LIPd and 2.2 ± 0.9 [mode: 2] μl for LIPv). The cannula was withdrawn 15 minutes after the completion of each injection. Injections were visible as bright halos representing the Mn-induced T1 signal increase.

Part of our motivation in developing the muscimol+Mn-MRI technique was to be able to detect any leakage of the drug along the injection track into regions distant from the intended injection site. Such leakage, which cannot be detected with traditional injection methods, limits the interpretation of all previous inactivation studies. In contrast, with the Mn-MRI technique, any significant leakage that occurs during cannula advancement and/or injection, or any backfilling that occurs during cannula retraction, is clearly visible in the post-injection MRI. An example of this is shown in Supplementary figure 9. Injections that showed any sign of leakage along the cannula track or that failed to show a visible halo were excluded from our data set.

Only a single site (LIPd or LIPv) was tested in each injection session. Typically one injection and two control sessions were performed each week. The order of injections into LIPd and LIPv was intentionally varied for each animal to avoid systematic biases, as follows (d=LIPd, v=LIPv): Monkey Q: v,v,v,d,d,d,d,v,d,v,v,d,d,v,v. Monkey W: v, v, v, d, d. Monkey G: d,d,d,d,d,v,v,d,d,v,v,v,v,v,d. We found only small and non-systematic changes in the injection effects as a function of session number (see Supplementary Information, section “No evidence for cumulative lesions”).

Behavioral tasks

Two male Macaca fascicularis and one male Macaca mulatta monkey performed a standard memory-guided saccade task[2] and a visual search task (adapted from Wardak et al.[13], [15]) in control and injection sessions. Memory trials began with the animal looking at a fixation point on a vertically mounted screen 16 cm from the animal. After 350 ms fixation, a peripheral target appeared for 150 ms in one of eight directions 20° from the fixation point. After a subsequent 1 to 1.6 s delay, the fixation light was extinguished and the animal had 500 ms to saccade to within 10° of the remembered target location. 150 ms after the eyes acquired the peripheral window, the target reappeared and a corrective saccade to within 5° was required. Early saccades (before fixation offset), late (> 500 ms), inaccurate (> 10° from target), or failed corrective saccades were counted as errors. A total of 240 correct saccades were obtained per experimental session. Memory reach trials were interleaved with the memory saccade trials, but they are not described in this report.

In the visual search task, after 800 – 1300 ms of central fixation, the fixation point was extinguished and a search array appeared. On two-thirds of trials a purple square and 7 equally-spaced purple distractors with 3 different shapes appeared at 12° or 15° eccentricity. On one-third of trials the target appeared without distractors. Animals were rewarded for directing a single saccade to within 6° of the target. Trials were terminated if the animal saccaded to a distractor or made more than one saccade. A total of 144 trials without distrators and 288 trials with distractors were obtained in each experimental session.

To test whether initial eye position would modulate lesion effects, two monkeys performed separate blocks of the saccade and search tasks using starting eye positions and visual stimuli five degrees to the right or left of straight ahead.

Because the effects of the muscimol might change over time, the first two animals (Q and W) performed multiple blocks of tasks, with each block (45 minutes) consisting of three tasks running sequentially. The three tasks were interleaved visual saccades and reaches, interleaved memory saccades and reaches, and visual search. Initial eye position (5° to the right or left of straight ahead) was alternated on each consecutive set. A total of six blocks of data were collected in each control and injection experiment, lasting 4 – 5 hours. The third animal (G) performed only a single block of interleaved memory saccades and reaches and a single block of visual search in each session. The first three injections were performed in monkey G before it was fully trained on the search task, and therefore only saccade data were collected in those three experiments.

Behavioral data analysis

Injection session data were compared with data from 2 – 4 control sessions from adjacent days within 2 weeks of the injection day, so that cumulative lesion effects would not bias our results (see also Supplementary Information, section “No evidence for cumulative lesions”). Errors that occurred prior to target appearance on memory and search trials were excluded from error analysis. Saccade errors include fixation errors (errors caused by eye movements, occurring at any time between the transient peripheral target presentation and the fixation point offset), target acquisition errors (failure to move the eyes to within 10° of

the remembered peripheral target location within 500 ms of fixation point offset), and late errors (failure to maintain fixation on the peripheral target for at least 150 ms, or a failure to make a corrective saccade to within 5° of the visible peripheral target location after it reappeared at the end of the trial). Search errors occurred when a saccade was landed more than 6° from the target, or when the first saccade was landed on a distractor. The saccade onset was defined as the time at which eye velocity first exceeded 30°/s, and saccade offset was defined as the time when eye velocity dropped below 24°/s. Movement amplitude was defined as the Euclidean distance from starting point to ending point. Precision was assessed by the variability of movement amplitude. To exclude oculomotor effects from the search task RT and error measurements, we subtracted no-distractor data from 7-distractor data, leaving only the influence of the distractors (adapted from Wardak, et al.[15]). For comparisons of reaction time (fixation offset to saccade onset, RT), amplitude and duration, we parceled out between-control-days and within-control-day variances, then used the control mean, the within-control-day variance, the injection mean, and the injection variance to compute two-sided Welch's t-test P values. For the comparison of the variability of movement amplitude (precision), we used the within-control-day variance and the injection day variance to compute two-sided F (variance ratio) test. We used two-sided chi-square tests (or Fisher exact tests if any of the expected counts were less than 5) for individual site error rate comparisons. Significant sites were the ones that significantly delayed RT or increased errors ($P < 0.05$, corrected for multiple comparisons of two). Population effects across injections were tested using a one sample two-sided permutation test. (Single sided tests would be appropriate for all of these comparisons, so the P values we report from the two-sided tests are generally conservative.) Unless otherwise mentioned, statistics were computed for the three contralateral target positions.

Image acquisition and analysis

Post-injection (4 – 8 hours) MR scans (T1 weighted, magnetization prepared rapid acquisition gradient echo [MP-RAGE] pulse sequences) were performed with a Siemens Allegra 3T MRI scanner (Siemens Medical Systems, Erlangen, Germany) using a custom volumetric ‘birdcage’ coil (14 cm inner diameter, Primatrix, Boston, MA). For about two thirds of the scans (25/35), animals were sedated (10 – 15 mg/kg ketamine and 0.7 – 1.0 mg/kg diazepam) or anesthetized with isoflurance and monitored using an MR-compatible pulse-oximetry probe (Surgivet). Ten scans were acquired while the animals were fully awake. Typically, three 8-minute scans at 0.5 mm^3 resolution were acquired with anaesthesia and six 3-minute scans at 1.0 mm^3 resolution were acquired without anaesthesia. See Supplementary Methods for image processing.

Injection depth was measured as the Euclidean distance from the center of each Mn halo to the adjacent gyral surface of the intraparietal sulcus, normalized by dividing by the full IPS sulcal depth (**Fig. 2**, inset) and multiplying by the mean full depth across the three animals (8.9, 17.6 and 12.0 mm respectively, for a mean of 12.8 mm). All depths in the text have been normalized in this manner. Normalization had only a very small effect on the results, and the distinction between LIPd and LIPv injections was just as clear using non-normalized values. All depth measurements were made in the coronal plane. To locate the depth of the LIPd/v boundary in the Lewis and Van Essen (2000) anatomical data, we first converted the

2-D fascicularis cytoarchitectonic parcellation into a 3-D volume (CARET, http://brainvis.wustl.edu, sum database: Macaque.F6.BOTH.Std-MESH.73730) and then computed the normalized depth of the border. We estimated the LIPd/v boundary as lying about 4.6 mm deep in the MRI atlas (full IPS depth: 8.7 mm) and 6.8 mm deep for the normalized sulcal depth of our animals (12.8 mm). All LIP injections were located near the middle of the IPS where the sulcus is relatively straight (e.g., **Fig. 2** inset), so sulcal curvature was not an issue in our measurements.

The normalized anterior-to-posterior distance (AP') for each injection was computed as the distance of the center of the manganese halo to the junction of IPS and POS (parietal occipital sulcus), relative to that animal's full anterior-to-posterior IPS length. These measurements were made in the horizontal plane.

Supplementary Material

Refer to Web version on PubMed Central for supplementary material.

Acknowledgements

We thank Justin Baker and Gaurav Patel for assistance in developing the Mn-MRI technique, and Thomas Malone, Jonathon Tucker, and Jason Vytlacil for technical assistance. This work was supported by NEI grant EY012135 and NSF (IGERT) grant 0548890. The content is solely the responsibility of the authors and does not necessarily represent the official views of the National Eye Institute or the National Institutes of Health.

References

1. Barash S, Bracewell RM, Fogassi L, Gnadt JW, Andersen RA. Saccade-related activity in the lateral intraparietal area. II. Spatial properties. J Neurophysiol. 1991; 66:1109–24. [PubMed: 1753277]
2. Snyder LH, Batista AP, Andersen RA. Coding of intention in the posterior parietal cortex. Nature. 1997; 386:167–70. [PubMed: 9062187]
3. Gottlieb JP, Kusunoki M, Goldberg ME. The representation of visual salience in monkey parietal cortex. Nature. 1998; 391:481–4. [PubMed: 9461214]
4. Bisley JW, Goldberg ME. Neuronal activity in the lateral intraparietal area and spatial attention. Science. 2003; 299:81–6. [PubMed: 12511644]
5. Thier P, Andersen RA. Electrical microstimulation distinguishes distinct saccade-related areas in the posterior parietal cortex. J Neurophysiol. 1998; 80:1713–35. [PubMed: 9772234]
6. Cutrell EB, Marrocco RT. Electrical microstimulation of primate posterior parietal cortex initiates orienting and alerting components of covert attention. Exp Brain Res. 2002; 144:103–13. [PubMed: 11976764]
7. Lynch JC, Graybiel AM, Lobeck LJ. The differential projection of two cytoarchitectonic subregions of the inferior parietal lobule of macaque upon the deep layers of the superior colliculus. J Comp Neurol. 1985; 235:241–54. [PubMed: 3998211]
8. Tanne J, Boussaoud D, Boyer-Zeller N, Rouiller EM. Direct visual pathways for reaching movements in the macaque monkey. Neuroreport. 1995; 7:267–72. [PubMed: 8742467]
9. Blatt GJ, Andersen RA, Stoner GR. Visual receptive field organization and cortico-cortical connections of the lateral intraparietal area (area LIP) in the macaque. J Comp Neurol. 1990; 299:421–45. [PubMed: 2243159]
10. Stanton GB, Bruce CJ, Goldberg ME. Topography of projections to posterior cortical areas from the macaque frontal eye fields. J Comp Neurol. 1995; 353:291–305. [PubMed: 7745137]
11. Rushworth MF, Nixon PD, Passingham RE. Parietal cortex and movement. I. Movement selection and reaching. Exp Brain Res. 1997; 117:292–310. [PubMed: 9419075]

12. Chafee MV, Goldman-Rakic PS. Inactivation of parietal and prefrontal cortex reveals interdependence of neural activity during memory-guided saccades. J Neurophysiol. 2000; 83:1550–66. [PubMed: 10712479]
13. Wardak C, Olivier E, Duhamel JR. A deficit in covert attention after parietal cortex inactivation in the monkey. Neuron. 2004; 42:501–8. [PubMed: 15134645]
14. Li CS, Mazzoni P, Andersen RA. Effect of reversible inactivation of macaque lateral intraparietal area on visual and memory saccades. J Neurophysiol. 1999; 81:1827–38. [PubMed: 10200217]
15. Wardak C, Olivier E, Duhamel JR. Saccadic target selection deficits after lateral intraparietal area inactivation in monkeys. J Neurosci. 2002; 22:9877–84. [PubMed: 12427844]
16. Posner MI. Orienting of attention. Q J Exp Psychol. 1980; 32:3–25. [PubMed: 7367577]
17. Land MF, Hayhoe M. In what ways do eye movements contribute to everyday activities? Vision Res. 2001; 41:3559–65. [PubMed: 11718795]
18. Kustov AA, Robinson DL. Shared neural control of attentional shifts and eye movements. Nature. 1996; 384:74–7. [PubMed: 8900281]
19. Corbetta M, et al. A common network of functional areas for attention and eye movements. Neuron. 1998; 21:761–73. [PubMed: 9808463]
20. Kowler E, Anderson E, Dosher B, Blaser E. The role of attention in the programming of saccades. Vision Res. 1995; 35:1897–916. [PubMed: 7660596]
21. Lewis JW, Van Essen DC. Corticocortical connections of visual, sensorimotor, and multimodal processing areas in the parietal lobe of the macaque monkey. J Comp Neurol. 2000a; 428:112–37. [PubMed: 11058227]
22. Lewis JW, Van Essen DC. Mapping of architectonic subdivisions in the macaque monkey, with emphasis on parieto-occipital cortex. J Comp Neurol. 2000b; 428:79–111. [PubMed: 11058226]
23. Medalla M, Barbas H. Diversity of laminar connections linking periarcuate and lateral intraparietal areas depends on cortical structure. Eur J Neurosci. 2006; 23:161–79. [PubMed: 16420426]
24. Cox DD, Papanastassiou AM, Oreper D, Andken BB, Dicarlo JJ. High-resolution three-dimensional microelectrode brain mapping using stereo microfocal X-ray imaging. J Neurophysiol. 2008; 100:2966–76. [PubMed: 18815345]
25. Koretsky AP, Silva AC. Manganese-enhanced magnetic resonance imaging (MEMRI). NMR Biomed. 2004; 17:527–31. [PubMed: 15617051]
26. Desimone R, Duncan J. Neural mechanisms of selective visual attention. Annu Rev Neurosci. 1995; 18:193–222. [PubMed: 7605061]
27. Schneider W, Schiffrin RM. Controlled and automatic human information processing: I. Detection, search, and attention. Psychol. Rev. 1977; 84:1–66.
28. Andersen RA, Bracewell RM, Barash S, Gnadt JW, Fogassi L. Eye position effects on visual, memory, and saccade-related activity in areas LIP and 7a of macaque. J Neurosci. 1990; 10:1176–96. [PubMed: 2329374]
29. Sereno AB, Maunsell JH. Shape selectivity in primate lateral intraparietal cortex. Nature. 1998; 395:500–3. [PubMed: 9774105]
30. Schall JD, Morel A, King DJ, Bullier J. Topography of visual cortex connections with frontal eye field in macaque: convergence and segregation of processing streams. J Neurosci. 1995; 15:4464–87. [PubMed: 7540675]
31. Murthy A, Thompson KG, Schall JD. Dynamic dissociation of visual selection from saccade programming in frontal eye field. J Neurophysiol. 2001; 86:2634–7. [PubMed: 11698551]
32. Moore T, Armstrong KM, Fallah M. Visuomotor origins of covert spatial attention. Neuron. 2003; 40:671–83. [PubMed: 14622573]
33. Moore T, Fallah M. Microstimulation of the frontal eye field and its effects on covert spatial attention. J Neurophysiol. 2004; 91:152–62. [PubMed: 13679398]
34. Muller JR, Philiastides MG, Newsome WT. Microstimulation of the superior colliculus focuses attention without moving the eyes. Proc Natl Acad Sci U S A. 2005; 102:524–9. [PubMed: 15601760]

35. Ignashchenkova A, Dicke PW, Haarmeier T, Thier P. Neuron-specific contribution of the superior colliculus to overt and covert shifts of attention. Nat Neurosci. 2004; 7:56–64. [PubMed: 14699418]
36. Gaymard B, Lynch J, Ploner CJ, Condy C, Rivaud-Pechoux S. The parieto-collicular pathway: anatomical location and contribution to saccade generation. Eur J Neurosci. 2003; 17:1518–26. [PubMed: 12713655]
37. Moore T, Armstrong KM. Selective gating of visual signals by microstimulation of frontal cortex. Nature. 2003; 421:370–3. [PubMed: 12540901]
38. Yang T, Shadlen MN. Probabilistic reasoning by neurons. Nature. 2007; 447:1075–80. [PubMed: 17546027]
39. Huk AC, Shadlen MN. Neural activity in macaque parietal cortex reflects temporal integration of visual motion signals during perceptual decision making. J Neurosci. 2005; 25:10420–36. [PubMed: 16280581]
40. Ben Hamed S, Duhamel JR. Ocular fixation and visual activity in the monkey lateral intraparietal area. Exp Brain Res. 2002; 142:512–28. [PubMed: 11845247]
41. Ben Hamed S, Duhamel JR, Bremmer F, Graf W. Representation of the visual field in the lateral intraparietal area of macaque monkeys: a quantitative receptive field analysis. Exp Brain Res. 2001; 140:127–44. [PubMed: 11521146]
42. Ipata AE, Gee AL, Goldberg ME, Bisley JW. Activity in the lateral intraparietal area predicts the goal and latency of saccades in a free-viewing visual search task. J Neurosci. 2006; 26:3656–61. [PubMed: 16597719]
43. Powell KD, Goldberg ME. Response of neurons in the lateral intraparietal area to a distractor flashed during the delay period of a memory-guided saccade. J Neurophysiol. 2000; 84:301–10. [PubMed: 10899205]
44. Ipata AE, Gee AL, Bisley JW, Goldberg ME. Neurons in the lateral intraparietal area create a priority map by the combination of disparate signals. Exp Brain Res. 2009; 192:479–88. [PubMed: 18762926]
45. Wardak C, Ibos G, Duhamel JR, Olivier E. Contribution of the monkey frontal eye field to covert visual attention. J Neurosci. 2006; 26:4228–35. [PubMed: 16624943]
46. Dias EC, Segraves MA. Muscimol-induced inactivation of monkey frontal eye field: effects on visually and memory-guided saccades. J Neurophysiol. 1999; 81:2191–214. [PubMed: 10322059]
47. Aizawa H, Wurtz RH. Reversible inactivation of monkey superior colliculus. I. Curvature of saccadic trajectory. J Neurophysiol. 1998; 79:2082–96. [PubMed: 9535970]
48. Li CS, Andersen RA. Inactivation of macaque lateral intraparietal area delays initiation of the second saccade predominantly from contralesional eye positions in a double-saccade task. Exp Brain Res. 2001; 137:45–57. [PubMed: 11310171]
49. Vuilleumier P, Schwartz S. Modulation of visual perception by eye gaze direction in patients with spatial neglect and extinction. Neuroreport. 2001; 12:2101–4. [PubMed: 11447315]
50. Pavani F, Ladavas E, Driver J. Gaze direction modulates auditory spatial deficits in stroke patients with neglect. Cortex. 2005; 41:181–8. [PubMed: 15714900]

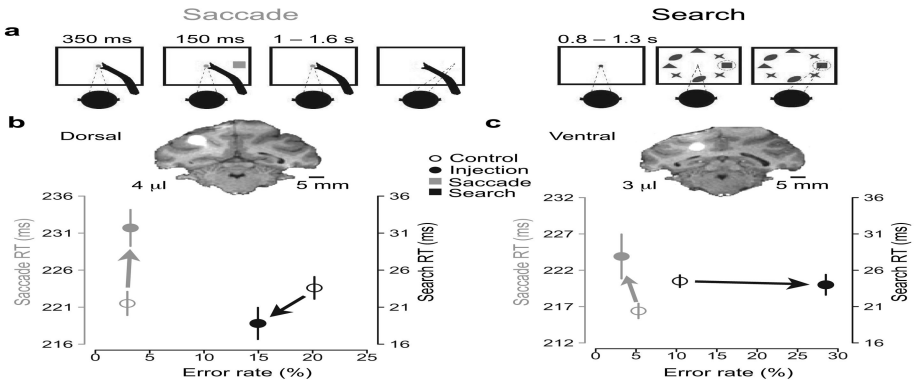

Figure 1. Behavioral tasks and example injections

a, Schematic of the memory-guided saccade and the visual search task. Saccades were directed to remembered target locations after a 1 – 1.6 s memory period. The visual search task was based on Wardak et al.[13], [15]: on two-thirds of trials, monkeys performed a single saccade directly to a purple target (a square) lying within a radial array of 7 purple distractors (ellipses, crosses, and triangles). On the other one-third of trials the target appeared alone, without distractors (not shown), as a control for the oculomotor effect. b + c, MRIs, reaction times (RT) and error rates from two example injections placed at different depths in the lateral bank of the IPS. Manganese mixed with muscimol resulted in a bright halo, seen here in coronal slices. Scale bars, 5 mm. The mean of saccade (grey) and search (black) RTs from each injection (solid circles) and their matched controls (hollow circles) are plotted against their corresponding error rates. Arrows show the effects of each inactivation in the RT and error rate domains. Upward and rightward directions indicate impaired behavior.

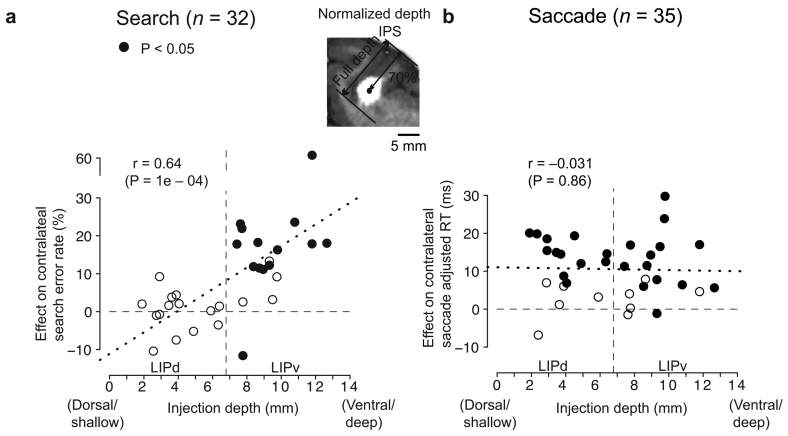

Figure 2. LIP lesion effects as a function of depth

a, Lesion-induced contralateral search error rate as a function of normalized injection depth. Inset illustrates how the full IPS depth and the lesion depth were measured for an LIPv injection from a coronal MRI slice. Filled circles represent injection sites with significant effects of either RT or errors ($P < 0.025$ prior to correction for the two independent comparisons). The vertical dashed line approximates the LIPd/v border. The mean LIPd effect was a change in error rate of −0.2 ± 1.4%, and the mean LIPv effect was 15.7 ± 3.4%. b, Contralateral adjusted saccade RT effect (see Supplementary Information) as a function of injection depth. Mean effects in LIPd and LIPv were 11.1 ± 1.8 ms and 10.1 ± 2.0 ms, respectively. See text for significance tests. Dotted lines are least-squares regression fits for the data, respectively. Four data points were shifted slightly to avoid overlap in a.

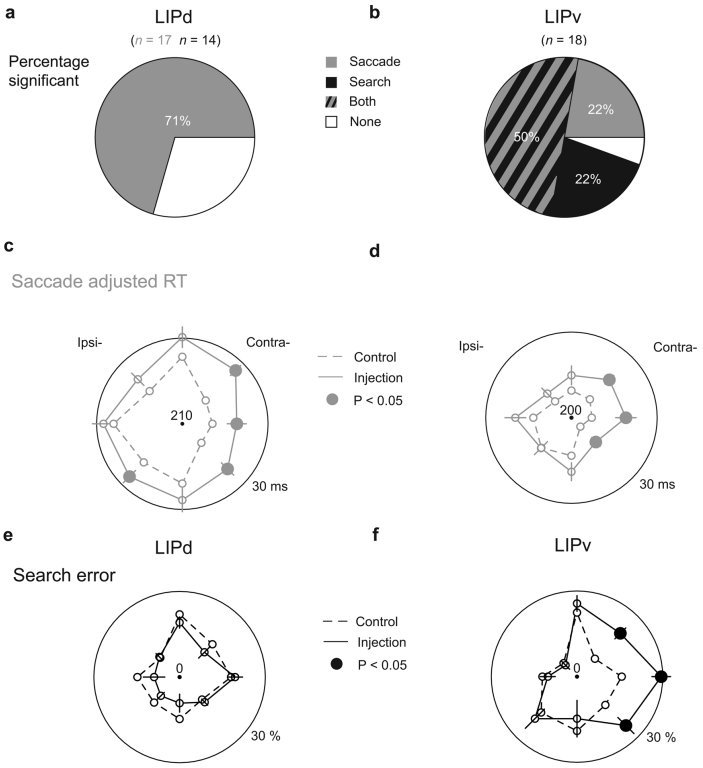

Figure 3. Performance of memory-guided saccades and visual search before and after LIPd and LIPv inactivations

a & b, Prevalence of significant saccadic (grey) and/or search (black) effects following LIPd and LIPv lesions. c – f, Mean adjusted saccade RT (grey) and search error rate (black) by target direction for LIPd and LIPv controls (dashed line) and injections (solid line). Large outer circles indicate 30 ms (saccade RT) or 30% (search error rate) beyond the center value. Error bars are ± 1 standard error of the difference between the control and injection values. Solid data points indicate significant effects ($P < 0.05$).

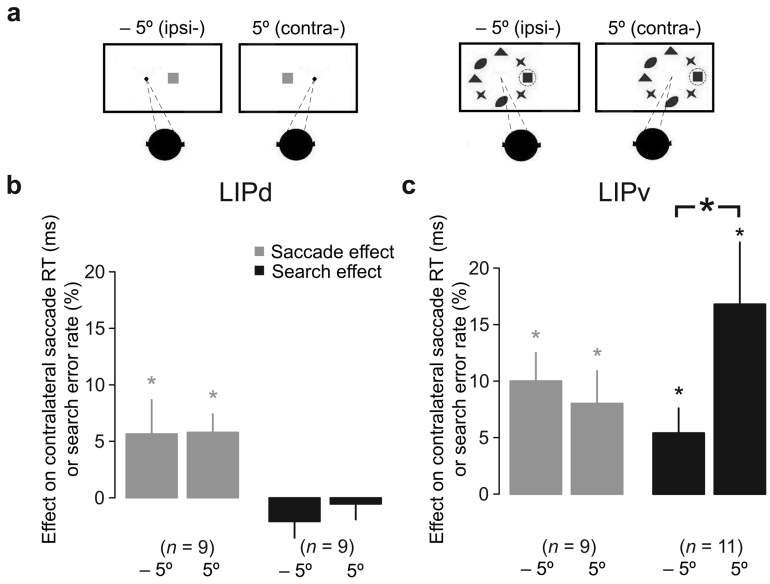

Figure 4. Initial eye position modulates search but not saccade effect

a, Initial eye position and all visual stimuli were displaced either 5° to the left or right for both memory-guided saccade task and visual search task. b & c, The mean effect with different eye positions on saccade RT (grey) and search error rate (black) in LIPd and LIPv. Error bars are one standard error of the mean; asterisks indicate $P < 0.05$.

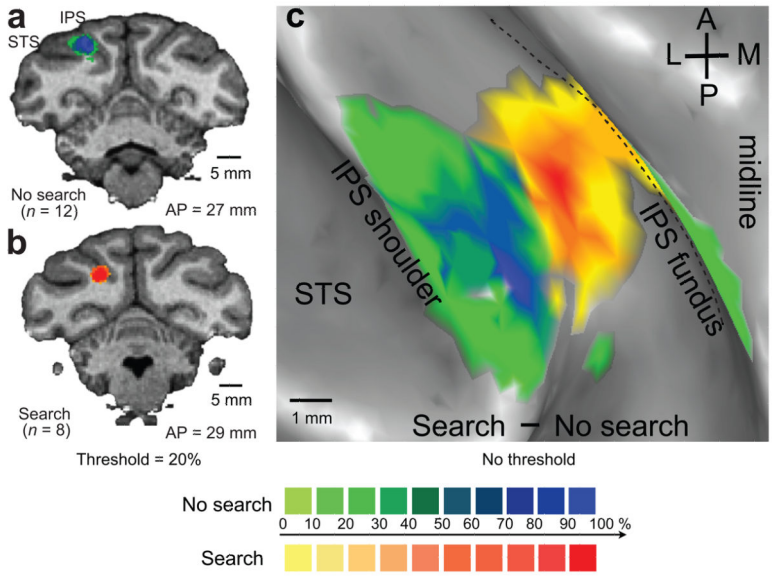

Figure 5. Lesion overlap maps

a & b. The estimated areas of inactivation (see Supplementary Information) for all search-negative (a) and search-positive (b) injections from two fascicularis animals shown on coronal brain slices. The color palette indicates the percentage of search-negative or search-positive lesions that involved each voxel. Data are thresholded at 20%. Scale bars, 5 mm. c. The voxelwise percentage effects from a and b were subtracted and projected, without thresholding, onto the inflated cortical surface. A, anterior; P, posterior; M, medial; L, lateral; IPS, intraparietal sulcus; STS, superior temporal sulcus. Scale bar, 1 mm.

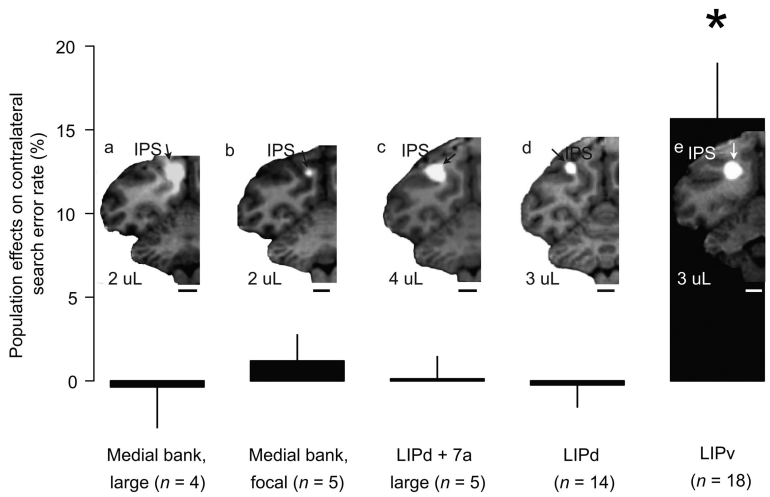

Figure 6. MRIs and search effects of control injections

Control injections were grouped into (a), large medial bank injections. (b), focal medial bank injections. (c), large LIPd + 7a injections. (d), LIPd. and (e), LIPv injections. Bars and error bars show the population effects of each injection type on search error rates in the contralateral hemifield. Error bars are one s.e.m.. Scale bars, 5 mm. Only LIPv injections produced a significant increase in search error rate. Data from the five large LIPd + 7a injections are included in the LIPd data shown in the rest of the paper.

Nat Neurosci. Author manuscript; available in PMC 2010 October 01.

Table 1

Effect of reversible lesions on saccade performance

Effect on saccade	Mean of G,Q & W		Monkey G		Monkey Q		Monkey W	
	RT	error	RT	error	RT	error	RT	error
LIPd: effect	7.1 ± 1.6 ***	4.2 ± 1.6 *	9.1 ± 2.9 *	5.7 ± 3.1	5.0 ± 2.1 +	4.5 ± 1.3 *	6.7 ± 1.9	−2.9 ± 1.0
% significant site	12 / 17 (70.6%)		7 / 8 (87.5%)		4 / 7 (57.1%)		1 / 2 (50%)	
LIPv: effect	7.3 ± 1.9***	2.9 ± 1.6 +	5.4 ± 2.6 +	5.2 ± 3.1	6.9 ± 3.4 *	3.2 ± 2.0	12.9 ± 4.1	−3.0 ± 2.3
% significant site	13 / 18 (72.2%)		6 / 7 (85.7%)		5 / 8 (62.5%)		2 / 3 (66.7%)	

Entries show mean ± standard deviation or percentage of sites that showed a significant increase in either contralaterally-directed saccade RT or error rate ($P < 0.05$, two-sided Welch's t-test for RT comparison and χ^2 test for error comparison, corrected for multiple comparison of two). Asterisks indicate significant effects:

*** $P < .001$;

** $P < .01$;

* $P < .05$;

+ $P < 0.1$.

Table 2

Effect of reversible lesions on search performance

Effect on search	Mean of G,Q & W		Monkey G		Monkey Q		Monkey W	
	% sig	mean	% sig	mean	% sig	mean	% sig	mean
LIPd	0 / 14 (0%)	−0.2 ± 1.4	0 / 5 (0%)	−0.3 ± 3.2	0 / 7 (0%)	−1.6 ± 1.6	0 / 2 (0%)	3.0 ± 0.9
LIPv	13 / 18 (72.2%)	15.7 ± 3.4 ***	5 / 7 (71.4%)	13.9 ± 1.7 *	6 / 8 (75%)	18.9 ± 7.4 *	2 / 3 (66.7%)	11.1± 4.4

Entries show mean ± standard deviation or percentage of sites that showed a significant increase in contralaterally-directed search error rate ($P < 0.05$, two-sided χ^2 test). Asterisks indicate significant effects:

*** $P < .001$;

** $P < .01$;

* $P < .05$;

+ $P < 0.1$.